Journal of Chromatography A, 1218 (2011) 849–855

Contents lists available at ScienceDirect

Journal of Chromatography A

journal homepage: www.elsevier.com/locate/chroma

Preparation and evaluation of a monolithic molecularly imprinted polymer for the chiral separation of neurotransmitters and their analogues by capillary electrochromatography

Bao-Yu Huang, Yu-Cheng Chen, Guan-Ren Wang, Chuen-Ying Liu *

Department of Chemistry, National Taiwan University, Taipei, Taiwan

ARTICLE INFO

Article history:
Received 28 September 2010
Received in revised form 8 December 2010
Accepted 10 December 2010
Available online 21 December 2010

Keywords:
Capillary electrochromatography
Chiral separation
Molecularly imprinted polymer
Monolith
Norepinephrine
Template

ABSTRACT

A monolithic molecularly imprinted polymer (MIP) column was prepared as the stationary phase for the capillary electrochromatographic (CEC) separation of a group of structurally related compounds including dopamine (DA), (±)-epinephrine (EP), (−)-isoproterenol (ISO), (±)-norepinephrine (NE), (±)-octopamine (OCT), and (±)-synephrine (SYN). Here, (−)-NE was used as the template. Either methacrylic acid (MAA) or itaconic acid (IA) together with a mixture of ethylene glycol dimethacrylate (EDMA) and α,α′-azobis(isobutyronitrile) (AIBN) in *N,N*-dimethylformamide (DMF) was introduced into a pre-treated, silanised, fused-silica capillary by a thermal non-covalent polymerisation procedure. Optimised conditions for the polymerisation reaction were assessed by the separation efficiency of the template. Both the template/monomer/cross linker molar ratio and the compositions of the functional monomer, cross-linker, and porogen affected polymerisation. The optimum *in situ* polymerisation reaction was performed at 65 °C for 17 min. By varying CEC parameters like eluent composition and pH, we observed that the addition of SDS to the eluent clearly improved the CEC separations. With a mobile phase of citrate buffer (10 mM, pH 3)/SDS (40 mM)/acetonitrile (2/2/1, v/v/v) solution and an applied voltage of 10 kV, the six related structures of the template and their enantiomeric mixtures were satisfactorily separated at 30 °C.

1. Introduction

Molecular imprinting allows synthetic polymers to be moulded into complementary binding sites for target molecules. The recognition properties displayed by molecularly imprinted polymers (MIPs) have been identified as robust selector phases in chromatography [1–3], solid phase extraction [4–6] and as receptors in chemical sensors [7]. Coupling the MIP technique to CEC takes advantage of the selectivity of MIPs and utilises the high efficiency of CEC [1,8–10]. This technique was first reported by Nilsson et al. in 1994 [11], and details on MIP-CEC methods and trends can be found in several review articles [12–15].

Among the different MIP formats for CEC, monolithic columns possess the advantages of easy preparation, versatile surface modification, good permeability and good peak capacity [2,15]. These unique merits have made monolithic columns attractive alternatives to the packed and open-tubular columns commonly used in separation sciences [8,10,16].

Enantioseparation is one of the most important separation techniques in various research fields, such as pharmaceutical, clinical, environmental and food science. MIPs have been shown by Nilsson's group to achieve high enantioselectivity when acting as chiral selectors [17–20], and chiral recognition applications of MIPs have also been reported [21,22]. Recently, a review article discussing the recent progress of chiral monolithic stationary phases in CEC and capillary LC was reported by Zhang et al. [2].

The neurotransmitters norepinephrine (NE) and epinephrine (EP), are both sympathomimetic agents with similar chemical structures. Both hormones are produced in the medulla and released by the adrenal glands, which cause vasoconstriction and blood pressure elevation [23,24]. To enantiomerically separate NE and EP with various modes of capillary electrophoresis, most work has operated with cyclodextrin or its derivatives [25–28]. Few attempts have used monolithic MIP/CEC mode chiral separation [29].

Herein, (−)-NE was used as template, and this monolithic MIP was employed as the CEC stationary phase for the recognition of a racemic mixture of NE, EP and their analogues. Considering that the synthesis of the polymeric monolith is the most important step in the application of a monolithic stationary phase [15,19,30–32], optimum conditions for the polymerisation reaction were investigated, including the template-to-functional monomer ratio and the

* Corresponding author at: Department of Chemistry, National Taiwan University, 1, Sec. 4, Roosevelt Road, Taipei 10617, Taiwan. Tel.: +886 2 33661645; fax: +886 2 23638543.
E-mail address: cyliu@ntu.edu.tw (C.-Y. Liu).

0021-9673/$ – see front matter © 2010 Elsevier B.V. All rights reserved.
doi:10.1016/j.chroma.2010.12.054

types of functional monomer, cross linker, and porogens. The surfactant, sodium dodecyl sulphate (SDS) has been shown to play a critical role in enantiomeric separations [22,33]. Schweitz et al. [34] reported the influence of surfactants on a MIP-CEC enantiomeric separation, but the addition of SDS decreased their efficiency. In our study, the effect of SDS on separation performance was also investigated, and SDS was found to increase the resolution of the analytes in a concentration-dependent manner, especially at higher temperatures.

2. Materials and methods

2.1. Instrumentation

All experiments were performed with a laboratory-built unit, consisting of a ±30 kV high voltage power supply (EH30P3, Glassman, USA) and a UV–VIS detector (SAPPHIRE 800 UV-VIS detector). Electrochromatograms were recorded and processed with a CT-21 (Peak-ABC, Singapore). The fused silica capillaries (Polymicro Technologies, Phoenix, AZ, USA) had a 75-μm i.d. and a 375-μm o.d. The total length of the capillary was 70 cm, with a distance of 50 cm between the injection and the detection window. The morphology of the prepared monolithic column was observed with an S-800 field emission scanning electron microscope (Hitachi, Tokyo, Japan).

2.2. Reagents and chemicals

All chemicals were of analytical reagent grade from Acros (Geel, Belgium) unless otherwise stated. Purified water (18 MΩ-cm) from a Milli-Q water purification system (Millipore, Bedford, MA, USA) was used to prepare all solutions. The following reagents were purchased as indicated: (−)-NE; (±)-NE; (−)-EP; (±)-EP; dopamine (DA); (±)-octopamine (OCT); (±)-synephrine (SYN); (−)-isoproterenol ((−)-ISO); *N*,*N*-dimethylacetamide (DMAC); *N*,*N*-dimethylformamide (DMF) and 1,1-diphenyl-2-picrylhydrazyl hydrate (DPPH) from Sigma (St. Louis, MO, USA); 3-trimethoxysilylpropyl methacrylate (γ-MPS) from TCI (Tokyo, Japan); methacrylic acid (MAA) from Lancaster (Lancashire, UK); α,α′-azobis(isobutyronitrile) (AIBN) from Wako (Osaka, Japan); acetic acid, sodium acetate anhydrous and mesityl oxide from Merck (Darmstadt, Germany); and itaconic acid (IA) from Fluka (Seelze, Germany). Stock solutions of the analytes (5 mM) were prepared in pure water and stored in a refrigerator. They were diluted accordingly prior to use. All solvents and solutions for CEC analysis were filtered through a 0.45-μm PTFE (Millipore).

2.3. Column preparation

Prior to the synthesis of the monolithic column, the fused silica capillary was rinsed with 0.1 M NaOH for 30 min, then with water for an additional 30 min. Next, the capillary was flushed with 0.1 M HCl for 30 min and water for an additional 30 min. The capillary was dried under nitrogen gas flow overnight at 110 °C. Silanisation of capillary columns has been previously described [8]. Before polymerisation, the silanised column was purged with DMAC or DMF for 30 min to remove any unreacted reagent. The preparation protocol for the MIP monolith is given in Table 1, where different molar ratios of template/monomer/cross linker were tested. The template was removed by washing with a methanol/acetic acid solution (10:1, v/v), and the resultant products were kept at room temperature prior to use. The performance of each column was examined through the chiral separation of (±)-NE, and the result was expressed as *f*/*g* in Table 1. The resolution factor, *f*/*g* is defined as the ratio of the distances from a line connecting the peak to the valley between the peaks (*f*) and the corresponding line to the baseline (*g*) [19].

2.4. Capillary electrochromatography

Before analysis, the monolithic columns were preconditioned with running buffer. Between sample runs, the columns were rinsed with methanol, pure water and buffer for 1- or 2-min intervals. The samples were injected by siphon at a height difference of 10 cm for 5 s. The samples were monitored at 210 nm by the UV absorbance detector.

2.5. Control of capillary temperature

Temperature was controlled by air circulation. The entire system was thermostatic in an environmental test chamber.

3. Results and discussion

3.1. Preparation of the MIP monolith

The nature of the porogen not only affects the efficiency, but also the selectivity of the MIP monolithic column [32,35]. Here, column performance was evaluated by the separation of template's racemic mixture, and expressed as an *f*/*g* value (Table 1). Initially, methanol, ethanol, toluene, and tetrahydrofuran were tested as the porogen. However, the template was insoluble in these solvents. DMAC was found to have greater dissolution power for the template at a temperature of 70 °C over a 10 min run time. Shorter retention times and better enantioseparation efficiencies were also observed as the volume of DMAC increased from 1.2 to 1.6 mL in the polymerisation reaction (Table 1, Columns A to C). This behaviour may result from accessibility into the imprinted cavity increasing due to softening of the polymer structure. When DMF was used, the template dissolved completely at room temperature, and the resolution improved significantly (Column E). Unfortunately, the resolution became poorer as the amount of DMF increased.

3.1.1. MAA as the functional monomer

Functional monomers are responsible for the binding interactions in the imprinted binding sites. For non-covalent molecular imprinting protocols, the preferred template-to-functional monomer ratio is 1:4 or greater [35]. When the amount of MAA was increased from 0.40 mmol to 0.59 mmol, the molar ratio of the template/monomer/cross linker increased from 1:10:22 to 1:15:22 (Column G). However, more functional monomer did not give better recognition performance. Based on these results and the theory that more cross linker will give higher mechanical strength, greater rigidity of the polymer seemed necessary to enhance recognition ability [35].

In an attempt to increase rigidity, we increased the amount of EDMA from 0.90 mmol to 1.54 mmol (Column H, ratio of 1:10:38). This test resulted in a poorer resolution than did previous work, which could be a result of insufficient polymerisation duration. By increasing the polymerisation time from 14 to 17 min, the separation efficiency increased with an *f*/*g* value of 0.74 (Column I). Considering this result, we then increased the polymerisation time to 17 min using the best performance conditions (Column E), but the column occluded.

3.1.2. IA as the functional monomer

Itaconic acid (IA), or methylenesuccinic acid, has two carboxylate groups, and the IA polymer is readily biodegradable. By using IA as the functional monomer, the recognition ability of the resulting MIP could be predetermined because of higher charged functionalities [31]. Therefore, IA was used as the functional monomer with

Table 1
Preparation protocol for monolith MIP[a].

Column	Template ((−)-NE)	Functional monomer	Cross-linker, EDMA	Porogen	Molar ratio[b]	*f*/*g*[c]
A	6.84 mg (0.04 mmol)	MAA, 34 μL (0.40 mmol)	169 μL (0.90 mmol)	DMAC, 1.2 mL	1:10:22	–[d]
B	0.04 mmol	MAA, 0.40 mmol	0.90 mmol	DMAC, 1.4 mL	1:10:22	0.43
C	0.04 mmol	MAA, 0.40 mmol	0.90 mmol	DMAC, 1.6 mL	1:10:22	0.55
D	0.04 mmol	MAA, 0.40 mmol	0.90 mmol	DMF, 1.2 mL	1:10:22	–[d]
E	0.04 mmol	MAA, 0.40 mmol	0.90 mmol	DMF, 1.4 mL	1:10:22	0.74
F	0.04 mmol	MAA, 0.40 mmol	0.90 mmol	DMF, 1.6 mL	1:10:22	0.55
G	0.04 mmol	MAA, 50 μL (0.59 mmol)	0.90 mmol	DMF, 1.4 mL	1:15:22	–[d]
H	0.04 mmol	MAA, 34 μL (0.40 mmol)	290 μL (1.54 mmol)	DMF, 1.4 mL	1:10:38	–[d]
I	0.04 mmol	MAA, 0.40 mmol	1.54 mmol	DMF, 1.4 mL	1:10:38	0.74
J	0.04 mmol	IA, 52 mg (0.40 mmol)	169 μL (0.90 mmol)	DMF, 1.4 mL	1:10:22	0.88
K	8.50 mg, (0.05 mmol)	IA, 0.40 mmol	0.90 mmol	DMF, 1.4 mL	1:8:18	0.91
L	0.05 mmol	IA, 0.40 mmol	180 μL (0.95 mmol)	DMF, 1.4 mL	1:8:19	0.99
M	0.05 mmol	IA, 60 mg (0.46 mmol)	0.95 mmol	DMF, 1.4 mL	1:9.2:19	1.00

[a] Initiator: AIBN 2 mg (0.01 mmol); polymerisation reaction: column A–H, at 65 °C for 14 min; column I–M, at 65 °C for 17 min.
[b] The molar ratio of template/monomer/cross-linker.
[c] Characterisation: column 70 cm (50) × 75 μm; sample: 1 mM (±)-NE; applied voltage: 10 kV; mobile phase: citrate buffer (pH 3, 10 mM)/SDS (40 mM)/ACN, 2/2/1 (v/v/v) solution.
[d] Nonresolved.

a template/monomer/cross linker ratio of 1:10:22. As expected, improved separation efficiency was observed (Column J), but the level of efficiency was still not satisfactory. We then added more template to increase the number of recognition sites (Column K, 1:8:18). The *f*/*g* value raised to 0.91, but the columns clogged easily. In comparison, when we increased the amounts of cross-linker from 0.90 to 0.95 mmol (Column L, 1:8:19, *f*/*g* = 0.99) then increased the amounts of IA to 0.46 mmol (Column M, 1:9.2:19), complete separation of the template was achieved. In summary, optimum conditions for in situ polymerisation included 0.05 mmol of template, 0.46 mmol of IA, 0.95 mmol cross-linker and 1.4 mL of DMF with a reaction time of 17 min at 65 °C.

3.2. Characterisation

The morphology of the monolith MIP column prepared in a 75-μm capillary tube was observed by SEM. The continuous skeleton and relatively large pores of the resultant polymer can be seen in the cross-sectional image of the capillary column (Fig. 1a). Fig. 1b is an amplification of a portion of Fig. 1a, and the uniform, ball-shaped, fine particles grown within the capillary and the permeability of the column are shown in Fig. 1c.

Several neurotransmitters and their analogues were chosen to evaluate column performance, and their structures are shown in Fig. 2. MIP-IA generated a greater EOF than MIP-MAA at a similar pH (Fig. 3).

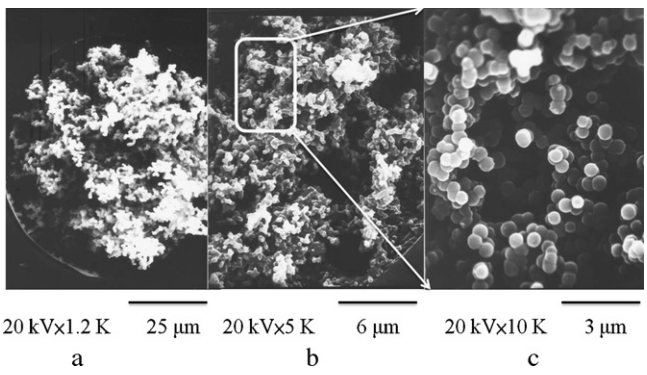

Fig. 1. SEM images of the monolithic MIP column. (a) A cross section of the capillary column, (b) an amplified image of (a), and (c) an amplified image of (b).

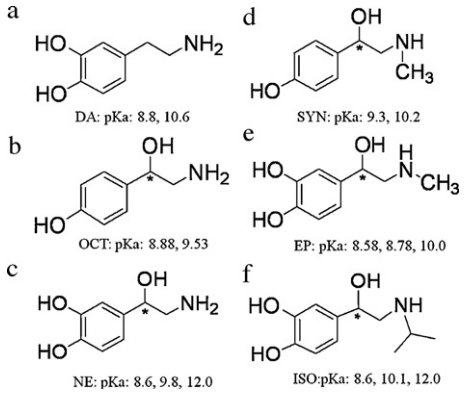

Fig. 2. The structures of the analytes and their dissociation constants. (a) Dopamine, (b) Octopamine, (c) Norepinephrine, (d) Synephrine, (e) Epinephrine, and (f) Isoproterenol. Physical data were from Ref. [39].

3.3. Optimisation of conditions for enantioseparation

3.3.1. Effect of pH

Eluent pH plays a critical role in CEC separation; it affects the molecular interactions between the MIP matrix and analyte and the retention of target analytes. Both MIP-MAA and MIP-IA gave similar retention patterns; as pH increased, retention times decreased. However, MIP-MAA only displayed a single peak for the enantioseparation of (±)-EP throughout the pH study: pH 3 at

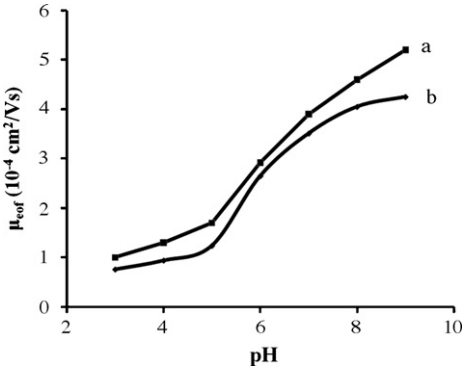

Fig. 3. EOF values at different pH values. Column 70 cm (50 cm effective length) × 75 μm; marker: mesityl oxide (1%); hydrostatic injection (10 cm, 5 s); mobile phase: phosphate buffer (10 mM); applied voltage: 10 kV; and detection wavelength: 210 nm. (a) MIP-IA and (b) MIP-MAA.

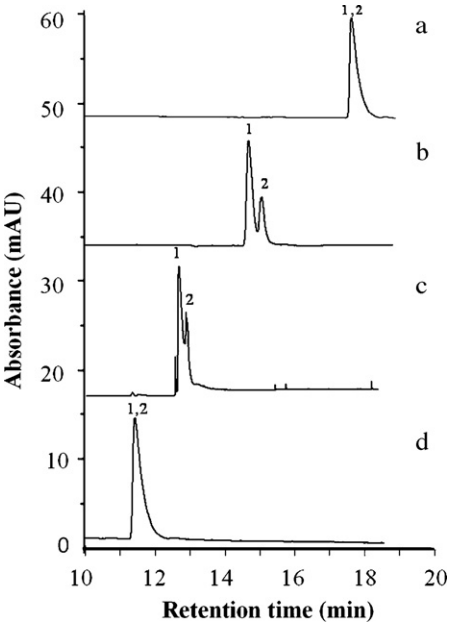

Fig. 4. Effect of pH on the chiral separation of (±)-EP. Conditions were as stated in Fig. 3, except for the following: a sample of (±)-EP (1 mM) and a mobile phase of acetate buffer (10 mM)/SDS (20 mM)/ACN (2/1/1) solution. Peaks: 1, (+)-EP; 2, (−)-EP. (a) pH 3.5, (b) pH 4.0, (c) pH 5.0, and (d) pH 6.0.

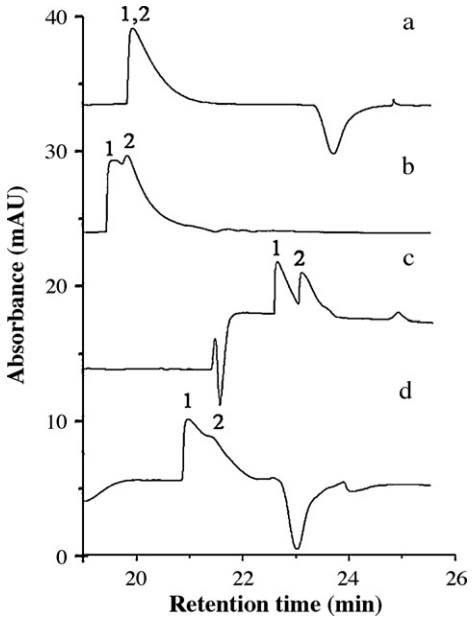

Fig. 5. The effect of mobile phase composition on the enantioseparation of (±)-NE. Conditions were as in Fig. 3, except for the following: a sample of (±)-NE (1 mM) and a mobile phase of a phosphate buffer (pH 4, 10 mM)/SDS (40 mM)/ACN solution in the volume ratios of (a) 5/4/1, (b) 5/3/2, (c) 5/2/3, and (d) 5/1/4. Peaks: 1, (+)-NE; 2, (−)-NE.

t_r = 20.2 min, pH 4 at 18.5 min, pH 5 at 12.0 min, and pH 6 at 7.6 min. The dissociation constant (pK_a) of MAA is 4.32, and those of IA are $pK_{a_1} = 3.85$ and $pK_{a_2} = 5.45$. Considering these values, the poor resolution observed with MIP-MAA may be due to lower electrostatic interactions between the analytes and the monobasic MAA monolith. Better separation efficiency was demonstrated with the dibasic IA monolith, especially at pH 4 (Fig. 4). However, as the pH increased, EOF increased because of the greater effective charge originating from the highly dissociated carboxylate groups in IA. This effect resulted in shorter retention times, which eventually led to poor resolution.

3.3.2. The effect of an organic additive

In general, the polarity and viscosity of the buffer solution are altered by the addition of an organic solvent; the EOF and electrophoretic mobility also change accordingly. To verify these effects in our system, the mobile phase was altered with 30%, 50%, and 80% acetonitrile by volume in a mixture of phosphate buffer (10 mM, pH 4.0) (Table 2). Unfortunately, no improvement in resolution was observed. A similar result was obtained when methanol was used in place of acetonitrile. However, the retention behaviour was different from that of acetonitrile; the retention affinity with the stationary phase increased as more methanol was added (Table 2).

3.3.3. Surfactant as an additive in the mobile phase

To increase hydrophobic interactions, various amount of SDS were added to the mobile phase (Tables 2 and 3, and Fig. 5). A strong adsorption between the protonated form of the analyte and the matrix was observed in acidic solution. In the presence of SDS, this adsorption was eliminated. Separation improved when the amount of surfactant was increased, which is possibly due to ion-pair formation between the analyte and SDS facilitating easier penetration into the cavities for molecular recognition. As the SDS concentration was increased to 60 mM, chiral resolution was lost. Better resolution occurred when the phosphate buffer (pH 4, 10 mM) containing SDS (40 mM) and acetonitrile had a volume ratio of 5/3/2 (Fig. 5b) and 5/2/3 (Fig. 5c). For our system, the presence of acetonitrile was therefore favourable over the range of 20–30% (v/v) in an SDS mixture. Kok and co-workers [36] showed that the highest selectivity in the CE separation of hydrophobic compounds was obtained with 20–40% (v/v) acetonitrile in an SDS mixture.

Comparatively, a cationic surfactant, CTAB was also tested in place of SDS. The critical micellar concentration (CMC) of CTAB is known to increase as more acetonitrile is added to the solvent [37], which could improve desirable hydrophobic interaction. Unfortunately, the addition of CTAB to similar conditions as SDS (10 mM, 25%, v/v) in an acetate buffer (10 mM, pH 4) was not found to have any effect on the chiral separation of NE or EP. The strong electrostatic attraction force of CTAB with the MIP-matrix may cause this poor recognition.

3.3.4. Types of buffer solution

When using phosphate buffer as the mobile phase, the MIP column was easily occluded after more than 200 injections. Hence, acetate, citrate and formate buffers were tested as replacements. Longer retention times were observed with acetate buffer, possibly due to the low ratio of the dielectric constant (ε) to viscosity (η) for acetic acid. It is understandable that complete resolution of the EP racemic mixture was achieved, while there was little resolution of the NE racemic mixture. The extra methyl group on EP makes it more hydrophobic and more inclined to interact with the MIP-matrix, eluting slower than NE.

Citrate buffer increased baseline stability. Compared to the other solutions tested. Complete resolution of the NE racemic mixture was achieved at pH 3.0, but not for EP (Fig. 6b). In this case, the low charge density environment of the MIP is similar to the prepolymerisation conditions for NE, where the complementary shape of the MIP cavities for the template molecules and a complicated solvent effect give good performance separation [38].

3.3.5. Concentration of the citrate buffer

As the concentration of citrate buffer increases (5–40 mM), the zeta potential and EOF decrease, increasing retention times. On the other hand, the affinities of the analytes for the MIP-matrix are known to lower as the ionic strength of the buffer increases. In a

Table 2
The retention behaviour of (±)-NE with different buffer compositions.

Buffer composition[a] (volume ratio)	Retention time (min) Peak 1; Peak 2	*f*/*g*
Phosphate buffer (PB)	18.87 (±2.34%)	–[b]
PB/ACN (7/3)	15.81 (±1.26%)	–[b]
PB/ACN (5/5)	12.27 (±1.47%)	–[b]
PB/ACN (2/8)	9.60 (±2.70%)	–[b]
PB/MeOH (7/3)	24.72 (±1.02%)	–[b]
PB/MeOH (5/5)	33.64 (±1.36%)	–[b]
PB/MeOH (2/8)	45.28 (±2.51%)	–[b]
PB/SDS (40 mM)/ACN (2/1/1)	15.15 (±2.40%); 16.63 (±2.69%)	0.74
Citrate buffer (CB)/SDS (5 mM)/ACN (2/2/1)	19.12 (±1.36%)	–[b]
CB/SDS (10 mM)/ACN (2/2/1)	17.79 (±1.42%); 18.54 (±2.03%)	0.52
CB/SDS (20 mM)/ACN (2/2/1)	24.89 (±2.01%); 25.50 (±2.42%)	0.68
CB/SDS (40 mM)/ACN (2/2/1)	21.27 (±1.97%); 26.50 (±1.76%)	0.91
CB/SDS (40 mM)/ACN (2/2/1)[c]	20.42 (±2.33%); 23.16 (±2.59%)	1.00

[a] PB: phosphate buffer (10 mM, pH 4); CB: citrate buffer (10 mM, pH 3).
[b] Nonresolved.
[c] MIP-M was employed; MIP-L was used for the others.

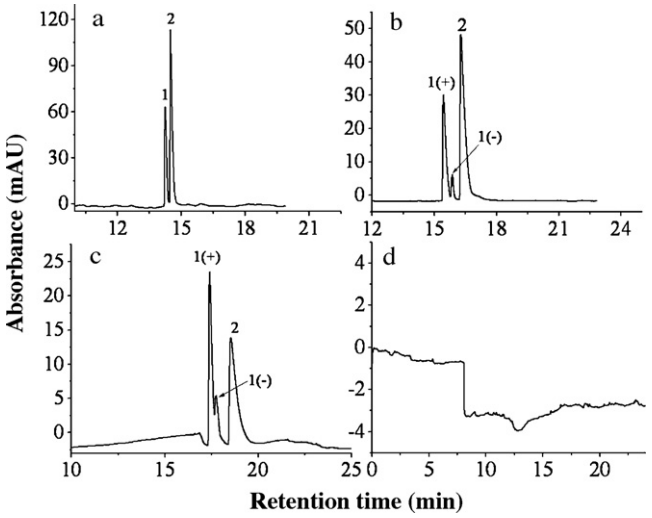

Fig. 6. Effect of citrate buffer concentration on separation. Conditions were as stated in Fig. 5, except for the following: a sample of (±)-NE (1 mM) and mobile phases of citrate buffer (pH 3, *x* mM)/SDS (40 mM)/ACN (2/2/1) solution, where (a) 5 mM, (b) 10 mM, (c) 20 mM, and (d) 40 mM. Peaks: 1, (+)-NE and (−)-NE; 2, (±)-EP.

complementary manner, only slightly longer retention times were observed as the citrate buffer concentration increased (Fig. 6). As the concentration was increased to 40 mM, an unstable baseline, and eventual loss of peak identification resulted (Fig. 6d). Hence, a concentration of 10 mM was chosen as the optimum concentration for further work.

3.3.6. The applied voltage

In the acetate buffer (10 mM, pH 4)/SDS (40 mM)/ACN (2/2/1, v/v/v) solution, the applied voltage changed from 5 to 20 kV (Table 3). The optimum condition for the chiral separation of EP was at an applied voltage of 10 kV.

3.4. Analytical application

3.4.1. Separation of the template structure-related compounds

Because of mutual interactions between the analytes, the enantiomeric separations of NE and EP could not be simultaneously performed within a single run. However, complete enantioseparation could be achieved separately (Figs. 4b vs. 6b). NE is a primary amine, while EP is a secondary amine. Greater hydrophobic interaction with the stationary phase was observed for EP, and it eluted after NE from the column. To gain a wider understanding of the prepared column, additional neurotransmitters and their analogues (Fig. 2) were chosen as model compounds to determine their retention behaviour. The retention order was as follows: DA < OCT < (+)-NE < (−)-NE < (+)-SYN < (−)-SYN < (+)-EP < (−)-EP < (−)-ISO (Fig. 7a). DA does not contain an asymmetric carbon, thus, it eluted the earliest. NE has one additional OH group compared to OCT, which created greater hydrogen bonding with the MIP matrix and caused it to elute after OCT. SYN

Table 3
Optimum conditions for the enantiomeric separation of (±)-EP.

Volume ratio[a] A[b] (*x* mM, pH 4)/B[c] (*y* mM)/ACN	Retention time (min)Peak 1; Peak 2	*f*/*g*
2 (10 mM)/2 (40 mM)/1	20.49 (±1.37%); 21.59 (±1.58%)	0.88
2 (20 mM)/2 (40 mM)/1	17.07 (±2.64%); 17.93 (±2.89%)	0.78
2 (30 mM)/2 (40 mM)/1	17.50 (±2.92%); 17.94 (±2.75%)	0.75
2 (40 mM)/2 (40 mM)/1	18.20 (±2.74%)	–[g]
2 (50 mM)/2 (40 mM)/1	18.60 (±3.10%)	–[g]
2 (10 mM)/1 (40 mM)/1	16.40 (±2.52%); 17.48 (±2.94%)	0.86
2 (10 mM)/1 (5 mM)/1	17.06 (±3.20%)	–[g]
2 (10 mM)/1 (10 mM)/1	16.33 (±2.44%); 17.27 (±2.11%)	0.34
2 (10 mM)/1 (20 mM)/1	24.49 (±2.81%); 25.64 (±2.64%)	0.88
2 (10 mM)/2 (40 mM)/1[d]	38.76 (±2.85%); 40.01 (±3.16%)	0.29
2 (10 mM)/2 (40 mM)/1[e]	12.50 (±2.20%)	–[g]
2 (10 mM)/2 (40 mM)/1[f]	9.00 (±3.47%)	–[g]

[a] The total volume of the mobile phase is 1.5 mL, applied voltage: 10 kV.
[b] Acetate buffer.
[c] SDS.
[d] Applied voltage: 5 kV.
[e] Applied voltage: 15 kV.
[f] Applied voltage: 20 kV.
[g] Nonresolved.

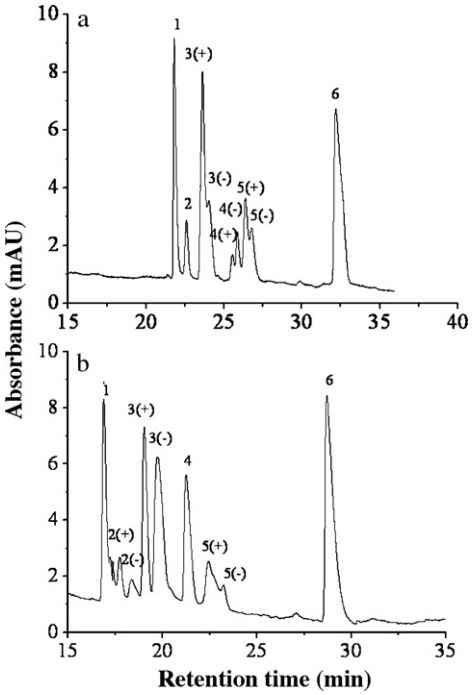

Fig. 7. Temperature effect on the separation of template structurally related compounds. Conditions were as stated in Fig. 5, except for the following: a column of MIP-M, sample concentrations of (−)ISO and (±)-EP at 0.5 mM and DA, (±)-OCT, (±)-SYN, and (±)-NE at 0.25 mM, and a mobile phase of a citrate buffer (pH 3, 10 mM)/SDS (40 mM)/ACN (2/2/1, v/v/v) solution. (a) 10 °C, and (b) 30 °C. Peaks: (a) 1. DA; 2. OCT; 3. (+)-NE and (−)-NE; 4. (+)-SYN and (−)-SYN; 5. (+)-EP and (−)-EP; 6. (−)-ISO; (b) 1. DA; 2. (+)-OCT and (−)-OCT; 3. (+)-NE and (−)-NE; 4. SYN; 5. (+)-EP and (−)-EP; 6. (−)-ISO.

has one extra methyl group compared to OCT, which creates a hydrophobic interaction with the MIP-matrix that slows the elution of SYN. Compared to NE, EP has one methyl substituent and ISO has one isopropyl substituent on an amino group. ISO eluted after EP.

3.4.2. Separation efficiency and stability of the column

The average separation efficiency of 9.8×10^4 plates/m was readily achieved with a column of 70 cm (50 cm effective length) × 75 μm ID, under an applied voltage of 10 kV, using a citrate buffer (pH 3.0, 10 mM)/SDS (40 mM)/ACN (2/2/1) solution, at a temperature of 30 °C and UV detection at 210 nm. The separation efficiencies of the individual analytes were as follows: DA, 1.4×10^5; OCT, 1.3×10^5; (+)-NE, 1.8×10^5; (−)-NE, 3.0×10^4; SYN, 6.0×10^4; (+)-EP, 5.0×10^4; (−)-EP, 1.8×10^5; and (−)-ISO, 5.0×10^4 plates/m.

The reproducibility and durability of separations are obvious important characteristics of a column. The RSD of the retention time for each column in three consecutive measurements are given in Tables 2 and 3. After long term use, the column will be slowly degraded. The type of mobile phase is an important factor in the stability of the three-dimensional structure of the cavity. During continuous use for two months, enantioseparation under the optimised conditions was still achieved over more than 600 injections.

Because thermal polymerisation was used in the column preparation, polymer could be expected to be present in the detection window. We have used UV transparent fused-silica capillaries as separation column with polymerization product present only prior to the detection window. We also used UV-transparent fused-silica capillary connected after the polymerised column as the detection window. No detection problems appeared to occur compared to column preparation without controls. Schweitz et al. [33] have also

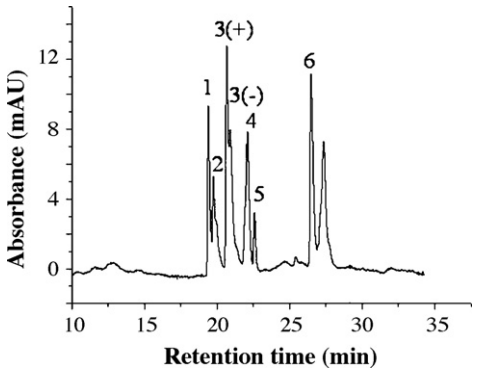

Fig. 8. The separation of analytes spiked into a urine sample. Conditions were as in Fig. 7(b), except that sample concentrations were 1 mM for (−)-ISO and (±)-EP, and 0.5 mM for DA, (±)-OCT, (±)-SYN and (±)-NE. Peaks: 1. DA; 2. (±)-OCT; 3. (+)-NE and (−)-NE; 4. (±)-SYN; 5. (±)-EP; 6. (−)-ISO.

reported the same phenomena in their review article. This might be only small amount of MIP in the detection window.

3.4.3. Effect of temperature

The effect of temperature on chiral separation was also investigated, and higher temperatures improved separation efficiencies significantly. With the exception of SYN, good chiral separation was observed at 30 °C (Fig. 7b). However, as temperature decreased to 10 °C, inadequate separation was observed. Unexpectedly, the resolution of SYN and EP improved at low temperatures.

3.4.4. Feasibility of the separation of a complex matrix sample

Analytes were spiked into urine to evaluate the separation of a complex matrix sample. The urine sample was filtered with a 0.45-μm syringe filter without further pre-treatments. Successful resolution for each of the six analytes and the enantioseparation of template molecule were obtained (Fig. 8). However, the urine's salt effect reduced the chiral separation power for some structurally related compounds.

4. Conclusions

In this work, a monolithic polymer with (−)-NE as a template was synthesised to perform chiral separations. Greater separation efficiency was observed when IA was used as the functional monomer, compared to MAA. The adsorption between the analytes and stationary phase was significant under acidic conditions. In the presence of SDS, resolution improved due to the formation of an ion-pair between analyte and surfactant. The optimum conditions for the enantioseparation of various neurotransmitters were found to be at a low pH with acetonitrile as the organic modifier, having a volume percentage of 20–30% in the mobile phase. The volume of SDS (20–40 mM) could not exceed 50% in the mobile phase; specifically, it could not surpass the critical micelle concentration value for the CEC system. Under acidic conditions, the citrate buffer performed the best in the chiral separation, while acetate buffer was the next most effective. Phosphate buffer is not recommended because the column was easily obstructed after long-term use.

Although the chosen analytes did not correspond to that of the template, the templated column can allow for different types of selectivity. It can be used for the separation of several structurally related analytes. These separations could be mediated by a combination of electrophoretic migration and chromatographic retention involving hydrophobic, hydrogen bonding, and electrostatic interactions within the cavity of the templated polymer. Conventionally, broadened peaks due to stronger interactions with the binding site have been shown for MIP columns, whereas, sharper peaks were

observed in the current study. The effect of temperature on chiral separation was also investigated. Higher temperatures were advantageous in the enantioseparations of most analytes, except for SYN and EP. No significant matrix effects were observed in the separation of these neurotransmitters and their analogues. Although the power of this enantioseparation technique in the analysis of a urine sample was not as good as using standard samples, the enantioseparation of the template molecules was still retained.

Acknowledgements

The authors thank the National Science Council of Taiwan for their financial support (Grant nos. NSC 95-2113-M-002 and NSC 96-2113-M-002-023-MY3).

References

[1] Z.S. Liu, C. Zheng, C. Yan, R.Y. Gao, Electrophoresis 28 (2007) 127.
[2] Z. Zhang, R.A. Wu, M.H. Wu, H.F. Zou, Electrophoresis 31 (2010) 1457.
[3] Y.P. Huang, Z.S. Liu, C. Zheng, R.Y. Gao, Electrophoresis 30 (2009) 155.
[4] M. Lasáková, D. Thiébaut, P. Jandera, V. Pichon, J. Sep. Sci. 32 (2009) 1036.
[5] P. Manesiotis, C. Borrelli, C.S.A. Aureliano, C. Svensson, B. Sellergren, J. Mater. Chem. 19 (2009) 6185.
[6] J. Haginaka, J. Sep. Sci. 32 (2009) 1548–1565.
[7] T.R. Ling, Y.Z. Syu, Y.C. Tsai, T.C. Chou, C.C. Liu, Biosens. Bioelectron. 21 (2005) 901.
[8] Y.C. Huang, C.C. Lin, C.Y. Liu, Electrophoresis 25 (2004) 554.
[9] S.C. Chuang, C.Y. Chang, C.Y. Liu, J. Chromatogr. A 1044 (2004) 229.
[10] C.C. Lin, G.R. Wang, C.Y. Liu, Anal. Chim. Acta 572 (2006) 197.
[11] K. Nilsson, J. Lindell, O. Norrlöw, B. Sellergren, J. Chromatogr. A 680 (1994) 57.
[12] L. Schweitz, L.I. Andersson, S. Nilsson, Anal. Chim. Acta 435 (2001) 43.
[13] J. Nilsson, P. Spegel, S. Nilsson, J. Chromatogr. B 804 (2004) 3.
[14] P. Spegel, L. Schweitz, S. Nillson, Electrophoresis 24 (2003) 3892.
[15] C. Liu, C. Lin, Electrophoresis 25 (2004) 3997.
[16] Z.S. Liu, Y.L. Xu, C. Yan, R.Y. Gao, J. Chromatogr. A 1087 (2005) 20.
[17] P. Spegel, L. Schweitz, S. Nilsson, Anal. Chem. 75 (2003) 6608.
[18] P. Spegel, J. Nilsson, S. Nilsson, Methods Mol. Biol. 243 (2004) 411.
[19] V.R. Mayer, Chromatographia 24 (1987) 639.
[20] L. Schweitz, P. Spegel, S. Nilsson, Analyst 125 (2000) 1899.
[21] N.M. Maier, W. Lindner, Anal. Bioanal. Chem. 389 (2007) 377.
[22] Y.L. Xu, Z.S. Liu, H.F. Wang, C. Yan, R.Y. Gao, Electrophoresis 26 (2005) 804.
[23] M. Castro-Puyana, R. Drewnowska, V. Pérez-Fernández, M.Á. García, A.L. Crego, M.L. Marina, Electrophoresis 30 (2009) 2947.
[24] S. Wei, G. Song, J.M. Lin, J. Chromatogr. A 1098 (2005) 166.
[25] C.E. Sänger-van de Griend, A.G. Ek, M.E. Widahl-Näsman, E.K.M. Andersson, J. Pharmaceut. Biomed. 41 (2006) 77.
[26] S.A.A. Rizvi, S.A. Shamsi, Electrophoresis 28 (2007) 1762.
[27] W.H. Henley, R.T. Wilburn, A.M. Crouch, J.W. Jorgenson, Anal. Chem. 77 (2005) 7024.
[28] B. Lin, Z.G. Shi, H.J. Zhang, S.C. Ng, Y.Q. Feng, Electrophoresis 27 (2006) 3057.
[29] G. Gübitz, M.G. Schmid, J. Chromatogr. A 1204 (2008) 140.
[30] P.R. Haddad, J. Chromatogr. A 1217 (2010) 901.
[31] M. Lu, Q. Feng, Q. Lu, Z. Cai, L. Zhang, G. Chen, Electrophoresis 30 (2009) 3540.
[32] M. Li, X. Lin, Z. Xie, J. Chromatogr. A 1216 (2009) 5320.
[33] L. Schweitz, P. Spégel, S. Nilsson, Electrophoresis 22 (2001) 4053.
[34] L. Schweitz, L.I. Andersson, S. Nilsson, Analyst 127 (2002) 22.
[35] P.A.G. Cormack, A.Z. Elorza, J. Chromatogr. B 804 (2004) 173.
[36] R.M. Seifar, J.C. Kraak, W.T. Kok, Anal. Chem. 69 (1997) 2772.
[37] Z. Lin, F. Yang, X. He, X. Zhao, Y. Zhang, J. Chromatogr. A 1216 (2009) 8612.
[38] A. Berthod, Anal. Chem. 78 (2006) 2093.
[39] C.J. Drayton, Comprehensive Medicinal Chemistry, vol. 6, Pergamon Press, Oxford, 1990.